American Mineralogist, Volume 93, pages 1886–1898, 2008

The parental melt of lherzolitic shergottite ALH 77005: A study of rehomogenized melt inclusions

Christina Calvin* and Malcolm Rutherford

Department of Geological Sciences, Brown University, Providence, Rhode Island 02912, U.S.A.

Abstract

Lherzolitic shergottite ALH 77005 is one of the most primitive martian meteorites. To characterize the parental melt of this primitive meteorite, olivine and chromite-hosted melt inclusions have been experimentally rehomogenized. The rehomogenization was performed with hydrostatic pressures (800–1000 bars) of CO_2 + CO gas along with finely powdered graphite at temperatures of 1150–1185 °C. Equilibrium between the host and inclusion melt was determined based on the lack of zonation in the host surrounding the melt inclusion, equilibrium K_D values of host and melt inclusions, and textures of the melt inclusion. Chromite-hosted melt inclusions, where chromite is poikilitically enclosed by olivine, contain ~7.5 wt% MgO. This composition most closely reflects the parental melt of ALH 77005. The melts trapped in Fo_{75} olivine contain ~7.1 wt% MgO when brought to equilibrium with the host. This olivine-hosted melt inclusion composition has lower SiO_2 (~50 vs. 53.9 wt%) and higher Cr_2O_3 (~1.2 vs. 0.2 wt%) and P_2O_5 (~1.2 vs. 0.5 wt%) than previous estimates for ALH 77005. In addition, compared with the chromite-hosted inclusions, the olivine-hosted ones have higher Al_2O_3 and lower CaO than can be explained through crystallization of phases known to be on the liquidus. This finding suggests that magma mixing occurred between chromite and olivine crystallization or olivine-hosted inclusions were contaminated by secondary minerals such as phosphate. Both olivine- and chromite-hosted melt inclusions in ALH 77005 have slightly higher Al_2O_3 than olivine inclusions in Chassigny but significantly higher Al_2O_3 than nakhlites such as MIL 03346 and Nakhla at similar values of MgO.

Keywords: ALH 77005, SNC meteorite, melt inclusion, parent melt, lherzolitic shergottite, olivine, chromite

Introduction

The Martian meteorite collection (SNC) has been studied extensively for clues to the nature and petrogenesis of igneous rocks on Mars (e.g., McSween 1985; Longhi and Pan 1989; Jagoutz 1991; Treiman 2003). One way these studies can provide information about martian magmatism is by characterizing the parental melts of the SNC meteorites. Defining the chemical characteristics of these magmas has the potential to provide important clues about the interior of Mars, processes involved in magma generation, the timing of these processes, and the relationship among the meteorites. However, the SNC meteorites comprise both mafic cumulate and basaltic igneous rocks, and the methods for determining the parental melt for cumulate and basaltic meteorites differ. For fine-grained basaltic shergottites such as Shergotty and Zagami, the quenched glass and phenocrysts are believed to have cooled in a closed system (e.g., Treiman 1986; McCoy et al. 1992; Wadhwa et al. 1994). Therefore, the bulk-rock compositions may represent the composition of the magma that erupted. In contrast, minerals present in cumulate meteorites, such as lherzolitic shergottite ALH 77005, have separated from the parental melt through processes such as crystal settling. The bulk rock of cumulate igneous rocks is not generally equal to the composition of the parent magma.

In the quest for parental magma compositions in cumulate meteorites, melt inclusions provide an alternative to studying interstitial melts, which are not preserved in these rocks. Melt inclusions form when melt is trapped by a growing crystal and is eventually cut off from the bulk of the magma (Roedder 1984 and references therein). Therefore, melt inclusions in cumulus minerals may provide a window into the crystallization history of a cumulate rock by trapping magma at various stages of parent magma evolution. If the crystal cools rapidly after entrapment, the trapped melt will quench to a glass. However, if the rock cools slowly, daughter crystals may begin to form within the melt inclusion and material may be added to or removed from the host phenocryst. To determine the parental melt compositions for cumulate SNC meteorites, several investigators have analyzed melt inclusions (e.g., Johnson et al. 1991; Ikeda 1998; Varela et al. 2000; Stockstill et al. 2002) through modal analysis of melt inclusion phases, defocused beam analysis, or rehomogenization using a heating stage. As will be discussed later, these methods present problems for slowly cooled igneous rocks and we have developed an alternative method for reestablishing crystal-melt equilibrium between a crystalline melt inclusion and the host phenocryst.

The focus of this study is on melt inclusions in lherzolitic shergottite ALH 77005. Based on the Fo content of olivines and the Mg number of melts found in the SNC meteorite collection, ALH 77005 is one of the most primitive martian meteorites

* E-mail: Christina_Calvin@brown.edu

and may provide insight into the petrology and composition of the primitive martian mantle. ALH 77005 contains two distinct textures (McSween et al. 1979; Lundberg et al. 1990). The first texture is composed chiefly of euhedral chromite and olivine, poikilitically enclosed by low-Ca pyroxene with minor interstitial maskelynite and high-Ca pyroxene (Fig. 1). The second texture consists of subhedral olivine with pyroxene, interstitial maskelynite, Ti-rich chromite, ilmenite, troilite, and merrilite. This paper focuses on the first textural domain in which chromites are found partially or completely enclosed by olivine suggesting that chromite crystallized early followed by olivine and then low- and high-Ca pyroxene. Chromites trapped in olivines, in low-Ca pyroxene, and in interstitial regions have four different zonation patterns depending on the host (Ikeda 1998). However, in general, the cores of chromites are Cr-rich ($\sim Chrm_{81}Sp_{14}Us_2Mt_3$) with increasing amounts of Ti and/or Al toward the rim. Olivine is unzoned in major element but the Fo content varies from 70 to 75 in different grains (Ikeda 1994). Orthopyroxene crystals have low-Ca, Mg-rich cores ($En_{74}Wo_6Fs_{20}$) that zone toward ferroan pigeonite rims ($En_{53}Wo_{25}Fs_{22}$). Textures and REE data suggest that plagioclase ($An_{52}Ab_{46}Or_2$) and whitlockite (or another phosphate) crystallized late in the sequence (Lundberg et al. 1990). Plagioclase has been largely converted to maskelynite by shock.

Chromite-hosted melt inclusions in ALH 77005 contain pyroxene and high-SiO_2 glass (Goodrich and Harvey 2002), however, no complete chromite-hosted melt inclusion compositions have been reported. Previous studies of this rock have instead focused primarily on olivine-hosted melt inclusions in the poikilitic lithology such as those in Figure 2 (Ikeda 1994, 1998; Zipfel and Goodrich 2001; Stockstill et al. 2002). Textural and chemical analysis of these melt inclusions highlights several interesting aspects of this meteorite. Some melt inclusions found in olivine are highly crystallized (Fig. 2a) and contain small (<5 μm), SiO_2-rich regions as well as crystals of high-Ca pyroxene and plagioclase (Jagoutz 1989; Ikeda 1998). Ikeda (1998) analyzed the major and minor elements of the phases contained in the olivine-hosted melt inclusions and used these data together with modal abundances to calculate a parental melt (melt inclusion composition) having between 54 and 60 wt% SiO_2 (Ikeda 1998). Recognizing that this composition was too silica-rich for an olivine-hosted melt inclusion, he added olivine host at various percentages to achieve a better estimate of the parental melt composition. Edmunson et al. (2005) looked at REE in olivine and olivine-hosted melt inclusions to identify possible causes of Sm-Nd disequilibrium in this meteorite. They concluded that Sm-Nd in olivine may have been altered by additions of impact melt. Based on studies of melt inclusions in ALH 77005, several authors have discussed the possibilities that these melt inclusions represent assimilated crustal material, remnants of mixed magmas, or immiscible melts (Harvey et al. 1993; Ikeda 1998).

In an effort to clarify the origin of these unusual olivine-

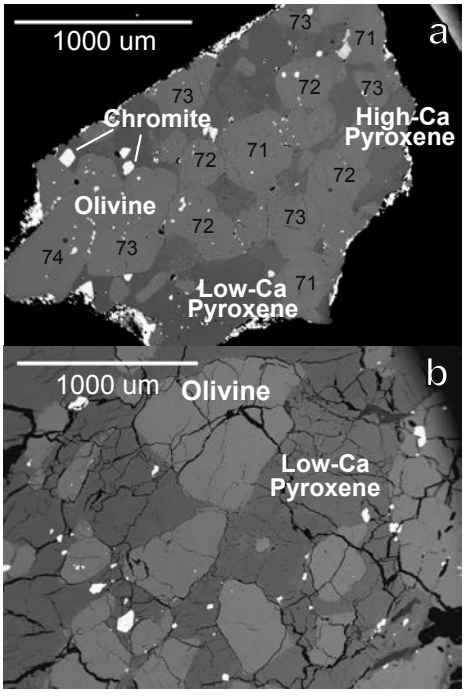

FIGURE 1. Back-scattered electron images of (**a**) an experimental chip of ALH 77005 (Exp. 4) and (**b**) thin section of ALH77005. White areas are chromite. Light-gray areas are olivine poikilitically enclosed in low-Ca pyroxene (dark gray). High-Ca pyroxene is also found interstitially. Forsterite contents of olivine are shown. Images confirm lack of Fe-Mg zoning determined from electron microprobe profiles. Variation in Fo contents between homogeneous grains indicates lack of late-magmatic or post-magmatic exchange between crystals.

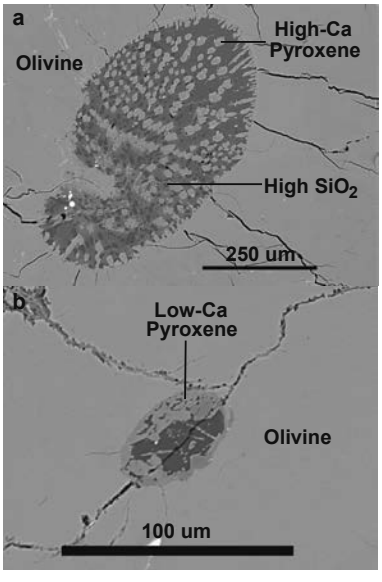

FIGURE 2. Back-scattered electron images of a thin section of ALH 77005 showing the two different types of olivine-hosted melt inclusions. (**a**) Large, highly crystallized melt inclusion with a very thin high-Ca pyroxene rim. The light-gray areas within the melt inclusions are also high-Ca pyroxene. The black spots are high-silica phases that may be quartz polymorphs. The interstitial region is glass. (**b**) Small melt inclusion with low-Ca pyroxene rim (light gray) along the outer margin of the melt inclusion. The dark-gray material in the interior is glass.

hosted melt inclusions and to better understand the nature of the parental magma of ALH 77005, we experimentally rehomogenized melt inclusions in olivine and chromite. Rehomogenization eliminates several potential problems in melt inclusion analysis by melting all of the daughter phases to form a homogenous glass that can then be analyzed. Analyses of rehomogenized glass inclusions eliminate sources of error that arise from analysis of a multiphase melt inclusion such as erroneous estimates of phase abundance, host-melt inclusion interactions, and zoning in small melt inclusion crystals. Determining the major- and minor-element composition of chromite- and olivine-hosted melt inclusions allows comparison of melts present during two early stages of the crystallization of this rock. The new melt inclusion data also allow comparisons between ALH 77005 primitive melt and those determined for other martian meteorites. Specifically, we compare ALH 77005 with melts with those determined for Chassigny and the nahklites MIL 03346 and Nahkla.

Experimental methods

Rehomogenization experiments were performed on 0.1 g chips of natural samples of ALH 77005 (ALHA77005,12). The chips of poikilitic-textured ALH 77005 were surrounded with packed graphite powder and sealed in platinum tubing. The graphite fixes the f_{O_2} at QFM –2.9 ± 0.1 for the experimental pressure (800–1000 bars) and temperature range used (1140–1185 °C) by allowing the terrestrially oxidized sample to react with carbon to achieve graphite-gas buffering (Eugster and Skippen 1967). This oxidation state is within the range estimated for shergottites by Wadhwa (2001) and Herd et al. (2002). The graphite also prevents the chips from reacting with the platinum sample tube that would result in Fe loss from the sample. The tubes were placed in TZM pressure vessels and brought to pressures of either 800 or 1000 bars. These pressures were chosen to fix the f_{O_2}, prevent incongruent melting of olivine to produce orthopyroxene and melt (Morse 1994 and references therein), and maintain the structural integrity of melt inclusions that had not been otherwise compromised by post-magmatic exchange of volatiles with the surrounding. The one disadvantage of this rehomogenization technique is that it precludes analysis of elements such as S that partition into the CO_2 + CO gas phase generated during the experiment. However, melt inclusions totally isolated within a host crystal may retain the original abundance of these elements, particularly for those that diffuse slowly in olivine and basaltic melt. No attempt was made to determine the H_2O in the homogenized melt inclusions in this study. ALH 77005, like all SNC samples, is highly shocked and fractured, and it is likely that volatile species such as H_2O were partially or completely lost during the shock event (Boctor et al. 2003). Additionally, ALH 77005 melt inclusions do not contain nominally hydrous phases such as amphibole. This feature is in contrast to Chassigny (Floran et al. 1978) and Nakhla (Treiman 1986), and suggests that the shergottite parent melt contained a lower abundance of water than has been estimated for the nakhlites and Chassigny (Watson et al. 1994).

Table 1. Experimental run conditions

Run no.	T	Pressure (in bars)	Time (in hours)	f_{O_2}	Mineral assemblage* (in olivine-hosted melt inclusions)
1b	1185	1000	3	QFM – 2.8	No inclusions
2	1185	1000	6	QFM – 2.8	No inclsusions
3	1150	1000	12	QFM – 2.7	plag, chrm, opx, cpx, si, phos, gl
4	1165	1000	72	QFM – 2.8	opx, gl
6	1165	800	23	QFM – 3.0	opx, gl
7	1160	800	24	QFM – 3.0	gl
8	1150	800	70	QFM – 2.9	opx, gl
9	1155	800	48	QFM – 2.9	No inclusions
11	1150	800	48	QFM – 2.9	opx, gl
12	1155	800	48	QFM – 2.9	opx, gl
13	1155	800	48	QFM – 2.9	No inclusions
14	1157	800	47	QFM – 2.9	gl
15	1140	800	72	QFM – 2.9	plag, opx, si, gl
17	1140	800	48	QFM – 2.9	opx, si, phos, gl

* Phases present are olivine = olv, low-Ca pyroxene = opx, high-Ca pyroxene = cpx, phosphate = phos, plagioclase = plag, high-Si phase = si, chromite = chrm, and glass = gl.

After pressurization, each chip was brought to temperature and held at the final pressure and temperature for 3 to 72 h (Table 1). Initial experiments were run for a relatively short duration. After the initial experiments, it was determined that experiments run for >24 h closely approached Fe-Mg exchange equilibrium between the olivine host and the melt inclusion. Samples were quenched by immersing the pressure vessel in H_2O. Thick sections were made using chips from the experiments that were polished until a melt inclusion was exposed. Once exposed, the melt inclusions were analyzed for major, minor, and some trace elements. The associated host and any daughter and/or rim minerals remaining in the inclusion were also analyzed for the same suite of major and minor elements. After analysis, thick sections were polished to expose new melt inclusions. Individual samples were polished and analyzed between 1 and 24 times.

Microprobe analyses were performed on a Cameca SX100 electron microprobe at Brown University. An accelerating voltage of 15 kV and a focused beam (1–2 μm) were used for all analyses. Glasses were analyzed with a 10 nA beam. The following standards were used to calibrate for glass standards: SiO_2, Al_2O_3, CaO, TiO_2, and FeO (basaltic glass VG-A99, USNM 113498), MgO (Kakanui hornblende, USNM 143965), Cr_2O_3 (chromite, USNM 117075), P_2O_5 (Al-phosphate, American Museum of Natural History), Na_2O (omphacite, USNM 110607), CaO (labradorite, USNM 115900), MnO (rhodonite, American Museum of Natural History), and K_2O (orthoclase, American Museum of Natural History). References to USNM standards can be found in Jarosewich et al. (1979). Because P_2O_5 was particularly high in these glasses and there was interference using the TAP crystal, analyses were done using the PET crystal (Mandeville 2004). Standardizations were checked using test analyses on basaltic glass VG-A99 (USNM 113498) and basaltic glass VG-2 (USNM 111240/52). Olivine and pyroxene were analyzed using a 15 nA beam and were calibrated using the following standards: SiO_2 and FeO (olivine Fo_{90}, USNM 111312/444,), MgO (olivine Fo_{83}, USNM 2566), Al_2O_3 (chrome-augite, benchstandard from Eugene Jarosewich at the Smithsonian Institution), CaO and Na_2O (omphacite, USNM 110607), MnO (rhodanite, American Museum of Natural History), TiO_2 (Kakanui hornblende, USNM 143965), Cr_2O_3 (chromite, USNM 117075), and K_2O (orthoclase, American Museum of Natural History). Standardizations were checked using test analyses on olivine Fo_{83} (USNM 2566) and chrome-augite (benchstandard from Eugene Jarosewich at the Smithsonian Institution).

Two polished thin sections of ALH 77005 were also used in this study: 117 and 54 from NASA Johnson Space Center in Houston, Texas. In addition, one chip of the natural sample (ALH 77005,12) was made into a thick section in an effort to develop a three dimensional picture of unhomogenized melt inclusions. The host phenocrysts, daughter crystals, glass matrix, and pyroxene rims associated with each melt inclusion were analyzed for major and minor elements using a Cameca SX-100 electron microprobe at Brown University.

Comparison of methods for investigating melt inclusion compositions

There are several techniques used for estimating the composition of partially or completely crystallized melt inclusions. Non-destructive techniques such as modal analyses and broad-beam microprobe techniques were reviewed in Roedder (1984 and references therein). Two destructive techniques have also employed: the heating-stage method (e.g., Sobolev et al. 1980; Zapunnyy et al. 1989) and rehomogenization in a 1 atm, gas-flow furnace (e.g., Zapunnyy et al. 1989; Gaetani and Watson 2000; Hauri 2002). Each of these techniques has advantages and drawbacks. In the case of ALH 77005, non-destructive techniques are particularly problematic as the size and highly crystallized nature of the melt inclusions often preclude getting an appropriate cross-section for accurate modal abundances of phases (Fig. 2).

A survey of existing rehomogenization techniques showed that they would not be the most appropriate for ALH 77005. Heating stage rehomogenization commonly uses the vapor bubble as a guide to completion of the rehomogenization (Danyushevsky et al. 2002 and references therein). As the daughter phases melt, the volume of the melt expands causing a decrease in the volume of the vapor bubble. However, consistent with previous melt inclusion analyses on SNC meteorites (Stockstill et al. 2005), melt inclusions in ALH 77005 rarely contain a vapor bubble as a guide for completion. In addition, any loss of the vapor phase after entrapment and cooling of the melt inclusion would change the remaining volume of the vapor phase and result in overheating of the melt inclusion during rehomogenization. As ALH 77005 suffered severe shock upon ejection from Mars, we suspect the vapor phase may have been lost from some inclusions (Johnson et al. 1991). Finally, analyses on a heating stage would be difficult if not impossible for highly fractured, sample material such as ALH 77005.

Rehomogenizing melt inclusions in a 1 atm, gas-flow furnace involves placing the sample in a furnace at a temperature above the liquidus for duration of ~10 min (Hauri 2002). The sample is immediately quenched. However, the kinetics of these reactions in coarsely crystallized melt inclusions such as those in ALH 77005 are slow and require longer durations in the furnace. Given the highly fractured nature of host crystals in ALH 77005, a high-pressure method was considered preferable.

The method we developed to rehomogenize melt inclusions under pressure takes into account the highly crystallized nature of the melt inclusions, the fragile nature of the sample, and the low f_{O_2} conditions at the time of crystallization. Our method fixes the oxidation state of the sample at a desired level based on the graphite-gas equilibrium and prevents exchange between the sample and the platinum container. The possible loss of some volatiles from the sample was a secondary concern to that of achieving crystal-melt equilibrium, and therefore we rehomogenized our melt inclusions in relatively long duration experiments. As will be explained later, textural and chemical criteria were used to make the determination of equilibrium between the trapped melt and host crystal.

RESULTS

ALH 77005 petrology

A thin section prepared from a chip of the same aliquot of ALH 77005 used in the experiments illustrates that it is predominantly composed of chromite and olivine poikilitically enclosed by low-Ca pyroxene (Fig. 1) as described by McSween et al. (1979). Although melt inclusions have been reported in olivine, chromite, and orthopyroxene, they are most common in olivine. No chromite-hosted melt inclusions were found in thin sections of the natural sample used for this study. Olivine-hosted melt inclusions that are magmatic in origin have undergone extensive crystallization and fall into two textural groups. One group consists of large (>100 μm diameter) inclusions with high- and low-Ca pyroxene and high-SiO_2 (>90 wt% SiO_2) daughter phases, whereas the other group consists of smaller (<50 μm) and considerably less crystallized inclusions, with low-Ca pyroxene rims adjacent to the olivine host and no other observable daughter phases (Fig. 2) (Ikeda 1998). In addition, our analyses have shown that, although pyroxene rims are formed adjacent to the inclusion-host contact in inclusions of both types, the large, highly crystallized melt inclusions have high-Ca pyroxene rims, whereas the small, crystal-poor melt inclusions have low-Ca pyroxene rims. One of the goals of melt inclusion rehomogenization was to determine what factors produce the two melt inclusion crystallization paths.

Results from rehomogenization experiments

Overview of experiments. Table 1 shows the run conditions for 14 rehomogenization experiments conducted on ALH 77005 chips. The first two experiments, performed at 1185 °C and 1000 bars for different periods of time, melted large portions of olivine, low-Ca pyroxene, and chromite to produce pockets of melt. It was determined that these experiments were run at too high a temperature to reasonably expect melt inclusions to remain isolated from these melt pockets. Subsequent experiments were run at lower temperatures and produced melt inclusions in various stages of rehomogenization depending on the temperature and run duration.

Olivine-hosted melt inclusions. Olivine melt inclusions analyzed after rehomogenization experiments were classified into one of three groups: partly homogenized with a variety of daughter crystals remaining in the melt inclusion; partly homogenized with only low-Ca pyroxene remaining visible in the melt inclusions; and nearly (or fully) homogenized melt inclusions that do not contain visible daughter crystals. Experiment 3, which was run at 1150 °C for 12 h, falls into the first category of olivine-hosted melt inclusions, and contained daughter phases of pyroxene, plagioclase, chromite, high-SiO_2 phases, and/or phosphates as well as pyroxene rims (Fig. 3a). The texture and compositions of the daughter phases mimic those in the natural thin section and these crystals are interpreted to be residual phases produced during melt inclusion crystallization that have not completely rehomogenized. Inclusions in experiments 4, 7, 8, and 11 fall into the second category. These melt inclusions contain euhedral pyroxene daughter crystals ($En_{74}Fs_{21}Wo_5$) but no longer retain pyroxene rims separating the host and melt (Fig. 3b). Finally, experiments 6, 12, 13, and 14 contain nearly or fully rehomogenized melt inclusions that do not contain visible rims or daughter crystals (Fig. 3c).

Comparisons of glass compositions from melt inclusions in various stages of rehomogenization (Fig. 4 and Table 2) reveal that with decreasing MgO (lower degrees of rehomogenization), SiO_2 increases while CaO and FeO decrease. At the same time, Al_2O_3 contents increase from 11 wt% to a peak at ~18 wt% (~3 wt% MgO) before beginning to decrease. Comparison of other major and minor elements shows that K_2O and Na_2O increase while FeO and TiO_2 decrease with decreasing MgO. There is a sharp decrease in FeO at below 4 wt% MgO. The amount of P_2O_5 increases with increasing MgO (rehomogenization), however, it is quite variable in olivine-hosted melt inclusions at MgO values of 6–7 wt%. As in the natural sample, individual host olivines exhibit no Fe, Mg, or Ca zoning (Table 3) but their Fo contents range from 70 to 75. Cr_2O_3 contents in olivine are <0.1 wt%. CaO, ranging between 0.13 and 0.23 wt%, is uniform within a single olivine crystal.

Chromite-hosted melt inclusions. Glass compositions of rehomogenized melt inclusions in chromite are shown in Table 4. All such melt inclusions were in chromites poikilitically enclosed in olivine and are free of daughter crystals. When compared with completely rehomogenized olivine-hosted melt inclusions, the chromite-hosted melt inclusions have higher MgO. Concentrations of SiO_2, Na_2O, FeO, K_2O, and TiO_2 are similar to olivine-hosted melt inclusions with MgO values between 6 and 7 wt%. CaO and P_2O_5 are slightly lower whereas Al_2O_3 is slightly elevated in chromite-hosted melt inclusions.

Chromite zoning is discussed extensively by Ikeda (1998) and will not be described here. However, minor zoning of chromite hosts at the margins of melt inclusions show increases in Al_2O_3 and TiO_2 (<1 wt%) and decreases in Cr_2O_3 (~3 wt%) at the host-melt inclusion contact. Figure 5 compares chromites analyzed in our experiments with those determined by Ikeda (1998).

DISCUSSION

Chromite-hosted melt inclusions: The parental magma of ALH 77005

Chromites poikilitically enclosed by olivine were the first crystallizing phase (McSween et al. 1979), suggesting that the parental melt composition of ALH 77005 may be best approximated by a chromite-hosted melt inclusion (Table 4). Compared with the olivine-hosted melt inclusions discussed in the following sections, chromite-hosted melt inclusions are less susceptible

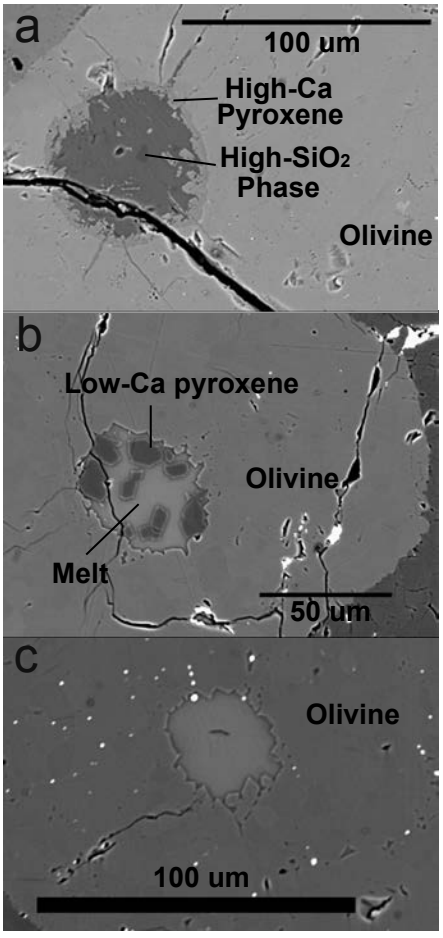

FIGURE 3. Back-scattered electron image of olivine-hosted melt inclusions in three experiments. (**a**) Melt inclusion that did not obtain equilibrium (12 h at 1150 °C). The rim is predominantly high-Ca pyroxene. Dark areas within the melt inclusion are high-silica phases surrounded by glass. (**b**) Melt inclusion that obtained olivine-melt equilibrium based on Fe-Mg exchange but did not fully rehomogenize. The dark-gray, euhedral crystals are daughter crystals of low-Ca pyroxene. (**c**) Fully rehomogenized melt inclusion that obtained equilibrium with its olivine host. The bright, spherical objects are quenched FeS-rich melts that were present in the sample prior to rehomogenization.

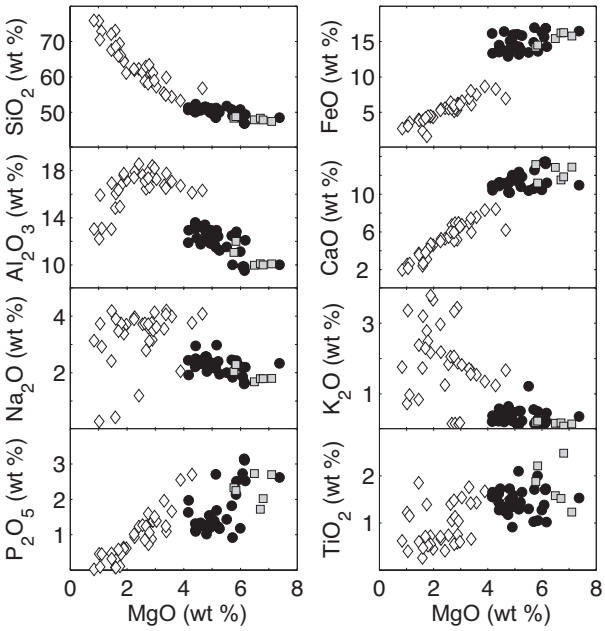

FIGURE 4. Glass compositions for olivine-hosted melt inclusions in various stages of rehomogenization. Open diamonds = melts from partially rehomogenized melt inclusions. These inclusions retain visible remnants of pyroxene rims, pyroxene daughter crystals, plagioclase, phosphates, and chromites. Solid circles = melt compositions from inclusions that retain only low-Ca pyroxene daughter crystals. Open squares = glass compositions from melt inclusions that show no visible daughter crystals and are interpreted to be nearly or completely rehomogenized and in equilibrium with their host olivine.

to post-entrapment effects such as reequilibration with the host and crystallization along the margin of the host-melt interface (Kamenetsky 1996). This feature is demonstrated in ALH 77005 by the preservation of distinct zoning patterns found in chromites enclosed by low-Ca pyroxene and olivine (Ikeda 1998).

Accordingly, we suggest that melt inclusion 7-10 reported in Table 4 represents the parental melt composition of ALH 77005 at the time of chromite crystallization. However, this composition has a Cr_2O_3 concentration of 1.35 wt%, which is anomalously high compared with terrestrial basalts and may reflect excess melting of the chromite host. The Cr_2O_3 contents of chromite-hosted melt inclusions are particularly sensitive to small changes in the melting of the chromite host because the Cr_2O_3 of the chromite is so much greater than the coexisting melt. Once chromite begins to crystallize in the ALH 77005 magma, the Cr_2O_3 of the melt begins to decrease (i.e., McCallum 1996), and thus the olivine-hosted melt inclusions trapped slightly later in the crystallization sequence are expected to contain lower Cr_2O_3. We have modeled possible corrections in the Cr_2O_3 (and other oxides) of the chromite-hosted melt inclusion using the Cr_2O_3 of olivine-hosted inclusions (0.2–0.4 wt%) as the lower limit to the melt trapped by chromite in ALH 77005. The results of these calculations are shown in Table 5. To reach the upper limit of Cr_2O_3 concentration observed in olivine inclusions, an excess of 1 and 2% of the chromite host would need to be remelted into the chromite inclusion. The recalculation to account for the excess Cr_2O_3 (1 wt%) in MI 7-10 increases the SiO_2 concentration of the parental melt by 1 wt%, CaO by 0.2 wt%, and decreases FeO by 0.2 wt%.

The recalculated chromite-hosted melt inclusion 7-10 (Table 5) is probably the best estimate of the parental melt for ALH 77005. This composition contains ~7.6 wt% MgO and 49.9 wt% SiO_2. The P_2O_5 in this melt (1.1 wt%) is an order-of-magnitude larger than previous estimates of either the parental melt or the melt inclusion compositions in ALH 77005. This high P_2O_5 is considered more reliable, as it is consistent with both the chromite- and olivine-hosted melt inclusions analyzed in this study. It suggests that the ALH 77005 magma is a partial melt

TABLE 2. Representative melt inclusion analyses

Experiment	3	3	4	6	7	8	12	std dev
Melt inclusion	3-11	3-12	4-5	6-1	7-7	8-2	12-2	
SiO_2	64.42	72.11	49.32	47.42	51.10	42.72	48.90	0.75
TiO_2	0.55	1.85	1.02	1.23	1.31	1.82	2.00	0.06
Al_2O_3	17.73	13.03	12.08	10.09	11.50	9.81	12.28	0.13
Cr_2O_3	0.02	0.02	0.04	0.28	0.02	0.17	0.09	0.02
FeO	4.49	3.99	14.29	15.79	16.51	15.22	14.28	0.14
MnO	0.07	0.09	0.47	0.51	0.44	0.37	0.39	0.81
MgO	1.89	1.45	6.17	7.10	5.90	7.07	5.84	0.13
CaO	4.72	3.72	11.21	12.86	10.23	14.84	10.89	0.11
Na_2O	3.38	2.41	2.19	1.80	2.44	1.60	2.27	0.17
P_2O_5	0.60	0.47	2.52	2.94	1.27	6.49	2.38	0.02
K_2O	3.78	0.84	0.46	0.15	0.14	0.31	0.27	0.03
Cl	0.02	0.07	not meas	0.47	0.09	0.66	0.17	
Mg number	43	39	43	44	39	45	42	
Total	101.65	99.98	99.77	99.98	100.03	99.23	99.78	
Host mineral	Olivine	Olivine	Olivine	Olivine	Olivine	Olivine	Olivine	
Host Mg number	73	74	75	73	70	74	71	
K_D (ol-melt)	0.26	0.22	0.27	0.27	0.26	0.27	0.30	
Daughter phases remaining	Pyroxene, Phosphate	Pyroxene, Plagioclase, Phosphate, Chromite	Low-Ca pyroxene	None	Phosphate	Low-Ca pyroxene, Phosphate	None	
No. of analyses	2	2	2	2	1	2	1	

Note: The first number in the melt inclusion number is the corresponding experiment's number.

TABLE 3. Representative host mineral compositions from experimental runs

Experiment	3	4	6	12	3	3
Host mineral	Olivine	Olivine	Olivine	Olivine	Cpx	Opx
SiO_2	37.93	38.24	37.80	37.85	51.80	55.14
FeO	23.13	22.08	23.08	25.08	8.13	13.90
MgO	37.95	38.31	37.92	36.50	16.96	27.27
Al_2O_3	–	–	–	–	3.05	0.45
Na_2O	–	–	–	–	0.31	0.03
MnO	0.60	0.57	0.49	0.51	0.36	0.57
TiO_2	–	–	–	–	0.60	0.07
Cr_2O_3	0.04	0.07	0.16	0.10	0.96	0.39
CaO	0.17	0.32	0.29	0.29	17.73	2.08
Mg number	75	76	75	72	79	78
Total	99.96	99.63	99.76	100.34	99.95	99.91

TABLE 4. Chromite-hosted melt inclusion compositions that best represent the parental melt composition of ALH 77005

Sample	7-1	7-10
T (in °C)	1160	1160
P (in bars)	800	800
Time (in hours)	24	24
SiO_2	50.22	48.96
TiO_2	2.35	2.79
Al_2O_3	11.28	11.79
Cr_2O_3	1.42	1.35
FeO	14.36	14.85
MnO	0.41	0.41
MgO	7.76	7.58
CaO	10.06	9.54
Na_2O	2.25	2.25
P_2O_5	1.29	1.10
K_2O	0.13	0.12
Sulfur (wt%)	0.16	0.10
Chlorine (wt%)	not meas.	0.07
Total	101.54	100.76
Host mineral	Chromite	Chromite
FeO	24.42	24.56
MgO	7.28	7.04
Al_2O_3	7.72	6.88
MnO	0.18	0.16
TiO_2	2.48	1.96
Cr_2O_3	56.95	59.05
Total	99.02	99.65

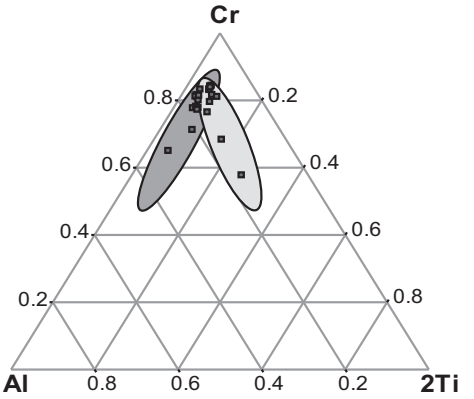

FIGURE 5. Plot of chromite compositions. Gray regions show two trends observed by Ikeda (1998). Black squares are analyses from this study, which are consistent the trends of Ikeda (1998).

of a cumulate zone that contained phosphates or an evolved trapped melt as well as olivine and low-Ca pyroxene (Borg and Draper 2003). The Cr_2O_3 for this parental melt (0.2 wt%) is also an order of magnitude larger than previous estimates for ALH 77005 olivine-hosted melt inclusions. The relatively high Cr_2O_3 in the parental melt indicates that the cumulate source of the magma may also have contained chromite.

Post-crystallization magmatic equilibration of major elements in ALH 77005

Before considering the results of the experiments with respect to olivine-hosted melt inclusions, it is necessary to address the possibility that olivine hosts and their entrained melt inclusions experienced significant reequilibration of Fe and Mg, and possibly minor elements, in post-entrapment magmatic events on Mars. Should such reequilibration have occurred, it may have significantly changed the composition of the melt inclusions. Of particular importance are Fe and Mg, which diffuse quickly through olivine relative to the other cations (Danyushevsky et

Table 5. Recalculated parental melt composition for chromite-hosted melt inclusion 7-10 (Table 3) and olivine-hosted melt inclusion 6-1 (Table 2) and the models assumed the host composition in adsorbed in ratios of 99:1, 98:2, and 97:3 (melt:host)

Mixing ratio	MI 7-10	99:1	98:2*	97:3	MI 6-1	99:1	98:2	97:3	96:4
SiO_2	48.96	49.45	49.94	50.43	47.42	47.33	47.23	47.14	47.04
TiO_2	2.79	2.80	2.81	2.81	1.23	1.22	1.21	1.19	1.18
Al_2O_3	11.79	11.84	11.89	11.94	10.09	9.99	9.89	9.79	9.69
Cr_2O_3	1.35	0.77	0.20	–0.38	0.28	0.28	0.28	0.27	0.27
FeO	14.85	14.75	14.66	14.56	15.79	16.05	16.32	16.58	16.84
MnO	0.41	0.41	0.42	0.42	0.51	0.51	0.51	0.51	0.51
MgO	7.58	7.59	7.59	7.60	7.1	7.22	7.34	7.46	7.57
CaO	9.54	9.64	9.73	9.83	12.86	12.73	12.61	12.48	12.35
Na_2O	2.25	2.27	2.30	2.32	1.8	1.78	1.76	1.75	1.73
P_2O_5	1.1	1.11	1.12	1.13	2.94	2.91	2.88	2.85	2.82
K_2O	0.12	0.12	0.12	0.12	0.15	0.15	0.15	0.15	0.14
Total	100.76	100.75	100.76	100.77	99.98	100.17	100.16	100.16	100.16

* Represents the chromite-hosted melt inclusion that most closely represents the parental melt based on the Cr_2O_3 concentration found in olivine-hosted melt inclusions.

al. 2000; Gaetani and Watson 2000, 2002). Significant exchange of Fe^{2+} and Mg^{2+} would produce either: (1) zoned olivine if reequilibration was not complete and the quench was rapid, or (2) neighboring olivine crystals with the same Fo content if the reequilibration occurred over an extended period of time. Consistent with previous studies of ALH 77005 (Ikeda 1994), we found that olivine in this rock is not zoned for any major elements but individual homogenous grains do vary from Fo_{69} to Fo_{75} within the same sample (Fig. 1). The fact that adjacent crystals retain different Fo contents indicates no late-magmatic event changed the MgO/FeO ratio subsequent to crystallization. The homogeneous nature of the olivines together with the grain to grain differences in Fo content does suggest that the grains were zoned at the time of entrapment in low-Ca pyroxene, and experienced diffusional reequilibration within each crystal. The grain to grain variability suggests that this reequilibration was limited to changes within the single grain and not to exchanges with other olivines or with a larger magmatic system.

Although there is also no detectable zoning in Al or Cr in ALH 77005 olivine, there is a prominent cyclic growth zoning of P (Fig. 6b). The formation of cyclic P zoning in olivine has been attributed to differences in growth rate in terrestrial olivines (Milman-Barris et al. 2008). Zones of fast-growing olivine incorporate higher P_2O_5 into their lattice compared with slow-growth cycles because the slow-moving, highly charged cations (P, Cr, V) concentrate around the growth front. This zoning can presumably develop without zoning of Mg in Fe that diffuse much more rapidly in the melt, but in this case, the crystals probably were zoned in Fe-Mg as discussed in the previous paragraph. The fact that the cyclic, growth-induced zoning is preserved in the natural sample and in the olivines after rehomogenization (Fig. 6d) supports our conclusion that ALH 77005 did not experience post-crystallization magmatic reequilibration.

Validation of rehomogenization technique

We have already addressed the necessity to develop a new technique for rehomogenizing melt inclusions in ALH 77005. However, to validate and understand the data obtained from rehomogenized melt inclusions in this study, two questions must be addressed. Did the melt inclusions achieve equilibrium with the host during the course of the experiment? And did they completely rehomogenize?

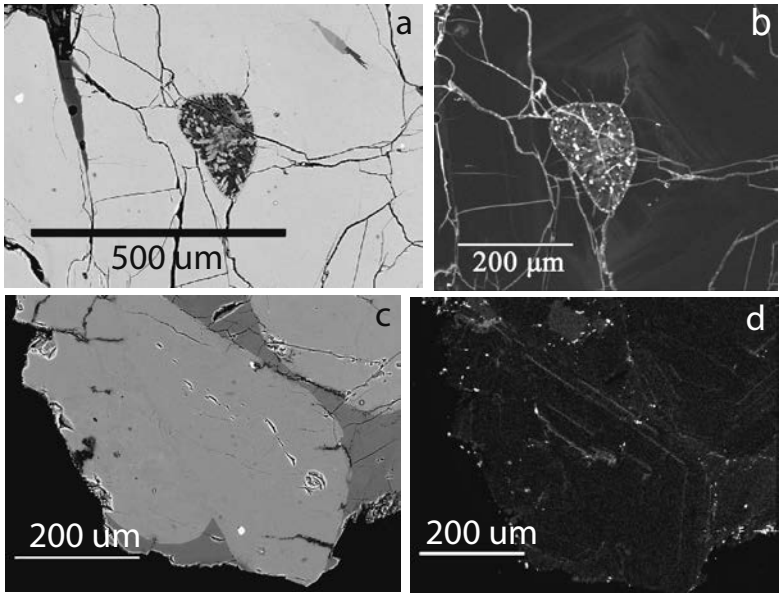

Figure 6. Comparisons of thin sections of the natural sample and thick sections of experimental samples. (**a**) Back-scattered electron image of an olivine-hosted melt inclusion in a thin section of the natural sample. (**b**) Phosphorus X-ray map of the same olivine-hosted melt inclusion in a thin section of ALH 77005. Bright areas are zones of high P_2O_5. The bright areas within the melt inclusion are phosphates that were either trapped with the melt or formed as the crystal grew. Oscillating zones of P_2O_5 content in the olivine may represent different growth rates of the olivine crystal (Milman-Barris et al. 2008). (**c**) Back-scattered electron image of an olivine (light gray) surrounded by low-Ca pyroxene (dark gray) in experimental sample CC1-05-3. (**d**) Phosphorus X-ray map of the same experimental sample. Phosphorus zoning was been preserved throughout the course of the experiment and defines the edges of the olivine grains.

Traditional melt inclusion rehomogenization techniques rehomogenize melt inclusions as quickly as possible to avoid exchange between the melt inclusion and the host (e.g., Frezzotti 2001; Danyushevsky et al. 2002; Hauri 2002). The short-duration heating in these experiments is based on two goals: (1) to find entrapment temperatures by observing changes in the vapor bubble over the course of reheating and (2) to avoid any diffusive exchange of major or minor elements between the host and the melt inclusion. We have made no attempt to determine the entrapment temperature here and therefore the first point is not relevant to this study. With regard to the second point, if the host changed composition after the melt inclusion was trapped, this chemical change could be transferred to the melt inclusion during rehomogenization. However, as discussed above, ALH 77005 olivine hosts appear not to have undergone major reequilibration after crystallization, and chromite hosts are particularly insensitive to changes in major and minor elements as the diffusion of most elements through the lattice is limited (Kamenetsky 1996). Therefore changes in the melt inclusion composition due to equilibration with the host over the course of the experiments are not a significant concern with ALH 77005.

Unlike other methods that require mathematical corrections to olivine-hosted melt inclusion compositions to account for Fe-Mg exchange with the host (Danyushevsky et al. 2000), the rehomogenization technique used in this study reestablishes the initial equilibrium between the trapped melt and the host phenocryst. Four criteria were used to determine equilibrium: the length of the experiment; texture of host and associated daughter phases; melt-olivine K_D; and the composition of coexisting olivine-hosts and low-Ca pyroxene daughter crystals. Only experiments that had been run for 48 to 72 h were considered as possibly achieving phase equilibrium. This period of time is long enough for MgO and FeO to reach diffusive Fe-Mg equilibrium in olivine (Danyushevsky et al. 2000; Gaetani and Watson 2000, 2002). In addition, for melt inclusions that retained daughter phases, equilibrium between the host, melt, and daughter crystals in the melt inclusions was interpreted to be approximated if the low-Ca pyroxene daughter crystals in the melt inclusion were euhedral. Olivine-hosted inclusions in our experiments that are texturally near equilibrium have a K_D in the range from 0.26–0.3 with most inclusions having a K_D of 0.27. The K_D for melts in equilibrium with olivine are generally near 0.30 (Roeder 1974), however, they can range from 0.25–0.35 since K_D varies with temperature, pressure, oxidation state, and composition (e.g., Mysen 1975; Ulmer 1989). Finally, the composition of the coexisting olivine and low-Ca pyroxene daughter crystals were compared for experiments that contained low-Ca pyroxene daughter crystals (Fig. 7). Tie lines connecting coexisting olivine, low-Ca pyroxene, and melt are shown as dashed lines. (The melt composition was normalized to the pyroxene quadrilateral so that it can be plotted along with the pyroxenes.) If the melt was out of equilibrium with the mineral phases, olivine would have diffusively reequilibrated faster than low-Ca pyroxene (Ganguly and Tazzoli 1994; Jurewicz and Watson 1988). The fact that the tie lines do not cross suggests that the melt, olivine, and low-Ca pyroxene approach compositional equilibrium in these experiments.

The second question to be addressed is whether any melt inclusions were completely homogenized. Of the ~100 olivine-hosted melt inclusions analyzed, only melt inclusions without daughter crystals could be considered completely homogenized. However, to identify whether the melt inclusion had fully homogenized or had been taken past homogenization by incorporating host material, we compared the compositions of olivine-hosted melt inclusion with those from chromite-hosted melt inclusions (Fig. 8; Tables 2 and 3), none of which contain visible daughter crystals. In Figure 8, the various oxides are plotted against MgO, which is a proxy for extent of crystallization. As discussed in the next section, the MgO content of the chromite-hosted melt inclusions is well constrained. Since the chromites are poikilitically enclosed in olivine, it is expected that they should have slightly higher MgO contents than their olivine counterparts, and this is the case.

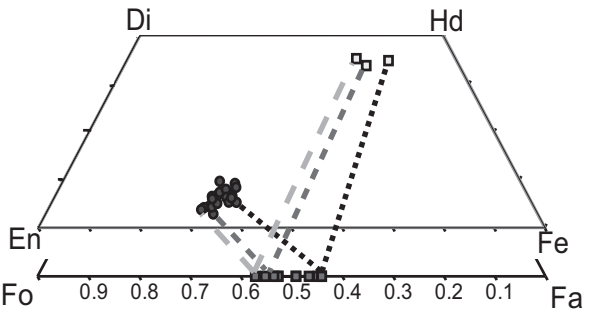

FIGURE 7. Coexisting pyroxene (circles), olivine (dark filled squares), and melt (light filled squares) compositions for minerals in equilibrium with melt at pressures ranging from 800–1000 bars and temperatures ranging from 1155 to 1165 °C and with f_{O_2} between QFM – 2.7 to QFM – 3.0. Melt composition was normalized to the pyroxene quadrilateral such that it would plot in the same location as a pyroxene with the same FeO-MgO-CaO ratio. Because the tie lines connecting these coexisting pairs do not cross, these phases were near equilibrium with each other.

To confirm these interpretations, we started with an olivine-hosted melt inclusion containing 7.1 wt% MgO and modeled its evolution as host olivine was remelted (Table 5). The results of this addition are shown in Figure 9 along with the analogous data for chromite remelting. Olivine was added to the olivine-hosted melt composition in increments of 1, 2, 3, and 4 wt%. After each increment, the Mg no. of the melt was allowed to equilibrate with the host olivine using a Fe-Mg K_D of 0.27. Given the relatively small volume of the melt inclusions (<300 μm), we treated the olivine as an infinite reservoir whereby the Mg no. of the host would not change. As already discussed, the compositional evidence suggests the olivine hosts were not significantly modified after entrapment. Therefore, we conclude that the melt trapped by ALH 77005 olivine phenocrysts is close to the composition reported here and it was unlikely to have been significantly modified by post-entrapment effects.

P_2O_5 in olivine-hosted melt inclusions

Several important points regarding the appearance of phosphate are revealed by comparing the compositions of olivine-hosted melt inclusions, as P_2O_5 shows significantly more variation at a given MgO than the other oxides (Fig. 10). Specifically, P_2O_5 is high in melt inclusions from experiments 8, 14,

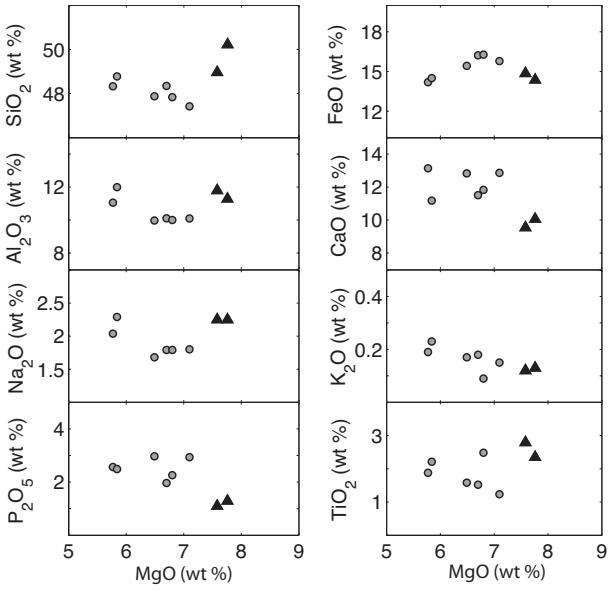

FIGURE 8. Composition of olivine-hosted melt inclusions (circles) that are nearly or completely rehomogenized (i.e., retain no observable daughter crystals) plotted along with chromite-hosted melt inclusions (triangles).

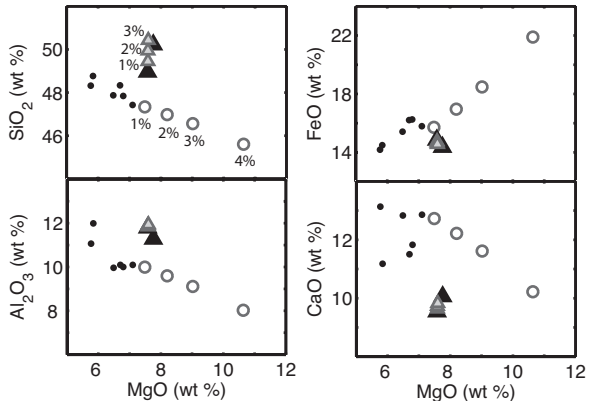

FIGURE 9. Compositions for rehomogenized olivine (solid circles) and chromite-hosted (solid triangles) melt inclusions. Host olivine is added into the olivine-hosted melt inclusion and allowed to reequilibrate. The open circles are a projection of melt composition as the host olivine was added to the rehomogenized melt in various percentages. Light gray triangles represent this projection of the chromite-hosted melt composition as chromite-host is added back into the melt in various percentages.

15, and 17. The variation in P_2O_5 at ~6 wt% MgO is positively correlated with CaO suggesting phosphates were incorporated into early crystallizing phases through one of three possible mechanisms. First, secondary phosphates found in cracks may have been mobilized during rehomogenization and incorporated into some melt inclusions. This would artificially raise the CaO and P_2O_5 in these inclusions. Second, P_2O_5 may be the result of olivine having incorporated a boundary layer at a fast-moving growth front. The components of the phosphates are trapped in melt inclusions as part of the boundary layer and saturate during cooling and crystallization within the melt inclusion. However, entrapment of the boundary layer should enrich other slow-diffusing cations such as Al and Ti in the inclusion but this is not observed. Finally, phosphates may have saturated prior to being incorporated into the melt inclusion. P_2O_5 diffuses slowly relative to other oxides in a natural silicate melt such that P_2O_5 may build up and apatite begins to nucleate and grow at the margin of a fast-growing phenocryst (Harrison and Watson 1984). X-ray maps for P of both natural and experimental samples show P zoning in olivine (Fig. 6), suggesting variation in olivine growth rate (Milman-Barris et al. 2008). The saturation of phosphates during olivine crystallization would be a significant departure from the crystallization sequence defined by Lundberg et al. (1990), who suggested that saturation of phosphates occurred at the end of the crystallization sequence.

Comparing olivine- and chromite-hosted melt inclusion compositions

The composition of the completely rehomogenized olivine and chromite-hosted melt inclusions differ significantly from each other in the case of some oxides (Fig. 8). For example, SiO_2 and Al_2O_3 are significantly lower, whereas CaO and P_2O_5 are higher in olivine-hosted melt inclusions than in chromite-

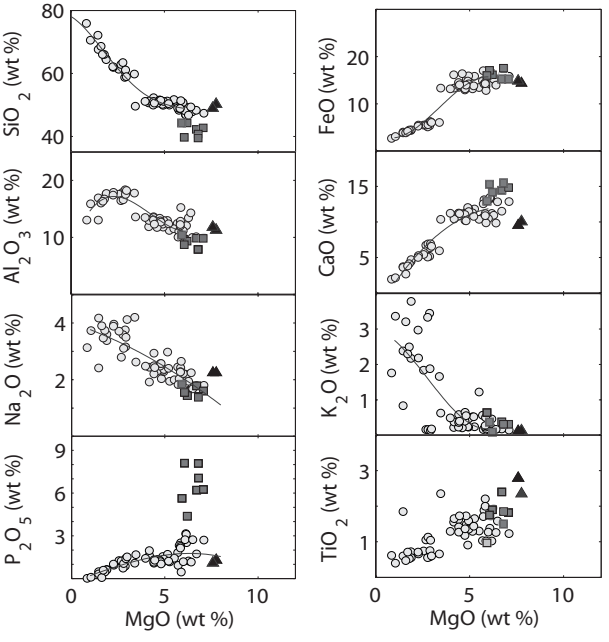

FIGURE 10. Chromite and olivine-hosted melt inclusions. Triangles represent the chromite-hosted melt inclusions. Olivine-hosted melt inclusions have been divided into high-P_2O_5 inclusions (squares) and those with lower P_2O_5 contents (circles). High-P_2O_5 melt inclusions are higher in CaO but lower in SiO_2 then low-P_2O_5 inclusions. The correlation with high CaO suggests that high-P_2O_5 melt inclusions contain re-melted phosphates. As the oxide contents are normalized to 100, SiO_2 contents of these melt inclusions are low as a result of having anomalously high P_2O_5 values in the melt. Errors for these analyses are smaller than the symbol size and can be found in Table 2.

hosted melt inclusions that differ by only 1 wt% in MgO (Fig. 8). Of specific interest are P_2O_5, CaO, and Al_2O_3, as they are not significant components in the only two phases known to be on the liquidus as the melt evolved from the chromite- to the

olivine-hosted melt inclusion composition. Figure 11 shows the evolution of the chromite-hosted melt inclusion composition assuming olivine and chromite crystallize in various percentages. It reveals that no percentage of chromite + olivine crystallization will produce a liquid line of descent that connects the magmas contained in chromite- and olivine-hosted inclusions. Even assuming crystallization of low-Ca pyroxene and plagioclase of the composition found in ALH 77005, there is no melt evolution path that brings the chromite-hosted melt inclusion composition to the olivine-hosted melt inclusions (Fig. 11). Even though Al_2O_3 is incorporated into chromite, it is incorporated in such small quantities that chromite crystallization cannot account for the lower Al_2O_3 observed in olivine-hosted melt inclusions.

This above discrepancy in melt inclusion composition may be explained by one or more magmatic processes including magmatic reequilibration of olivine, entrapment of a boundary layer during phenocryst growth, and magma mixing between chromite and olivine crystallization. It has already been shown that ALH 77005 olivine did not suffer significant modification of the Fe/Mg ratio, therefore the first possibility is considered unlikely. However, increasing MgO to the degree that it is consistent with chromite-hosted melt inclusions still produces an olivine-hosted melt composition that is inconsistent in Al_2O_3, CaO, P_2O_5, and SiO_2 with the melt trapped by chromite. If olivine and/or chromite-hosted melt inclusions trapped the boundary layer as they crystallized, slow-moving cations such as P could have been trapped in higher than average proportions. However, the slow-moving cations Al and Ti are too low in the olivine-hosted melt inclusions suggesting that the discrepancy cannot be solely attributed to this effect. Finally, the compositional difference may be evidence of injection of or mixing with a magma that is lower in SiO_2 and Al_2O_3. Several studies have already addressed whether ALH 77005 crystallized in an open or closed system (Lundberg et al. 1990; Harvey et al. 1993; Borg et al. 2002). Ikeda (1998) suggested that a high-K magma was introduced to the ALH 77005 magma during olivine crystallization but prior to low-Ca pyroxene crystallization. From our study of olivine-hosted melt inclusions, there does not appear to be a significant change in the K/Na ratio of olivine-hosted melt inclusions prior to the formation of plagioclase daughter crystals; however, our results could be explained by an injection of magma that is higher in CaO and P_2O_5 and lower in SiO_2 and Al_2O_3 between chromite and olivine-hosted melt inclusion entrapment.

A non-magmatic origin for this discrepancy could be contamination by phosphates that would artificially raise the P_2O_5 and CaO of the olivine-hosted melt inclusion composition. As discussed in the previous section, CaO and P_2O_5 enrichment in some inclusions may reflect secondary contamination by phosphates found in veinlets and cracks in the natural sample. If olivine-hosted melt inclusion compositions were modified to reflect the CaO and P_2O_5 content of the chromite-hosted melt inclusions, all other oxides would increase accordingly. Therefore Al_2O_3 and SiO_2 would increase such that they are consistent with the projected path of the melt composition assuming olivine crystallization (Fig. 11). After this correction, the only major oxide that does not become consistent between the two types of melt inclusions is FeO. As seen in Figure 8, the FeO concentration varied for olivine-hosted melt inclusions. This feature may reflect small changes in the Fe/Mg ratio of the magma during olivine crystallization. Olivine-hosted melt inclusions were in equilibrium with their olivine hosts; however, the Fo contents of the hosts ranged between 70 and 75. Therefore, the high FeO concentration of this particular melt inclusion may reflect a point in the magmatic evolution and entrapment where the MgO/FeO ratio had decreased.

Comparison of rehomogenized olivine-hosted melt inclusions with previous studies of ALH 77005

The purpose of experimentally rehomogenizing melt inclusions was to eliminate the effect of post-entrapment crystallization on our analyses. Comparing our results with previous melt inclusion studies of ALH 77005 (Table 6), it is clear that the experimentally rehomogenized olivine-hosted melt inclusion compositions have lower SiO_2 values (48 wt%) than most previous mode-based estimates. Unlike previous studies (McSween 1987; Jagoutz 1989; Harvey et al. 1993; Ikeda 1998), the SiO_2 contents of the olivine-hosted melt inclusions (~48 wt% SiO_2 at MgO of 6 wt%) from this study are demonstrated to be in equilibrium with a magma crystallizing olivine. In addition, the MgO content obtained by Ikeda (1998) is at least 4 wt% higher than the MgO content for the chromite melt inclusions obtained in this study (Table 4). As chromite was one of the first crystallizing phases and was co-crystallizing with olivine (McSween et al. 1979), it is unlikely that the olivine-hosted melt inclu-

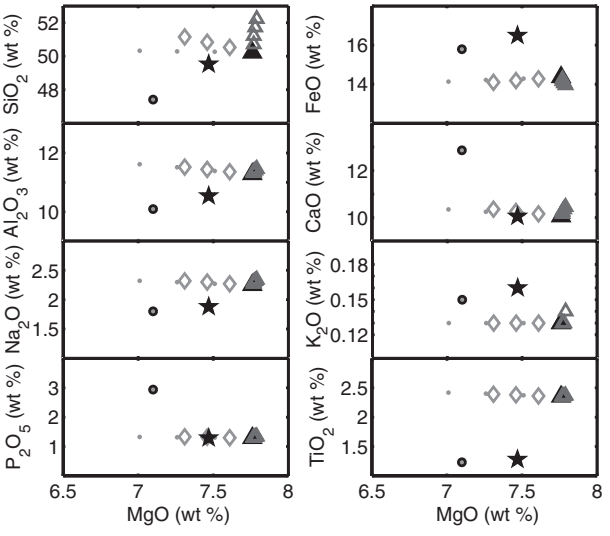

FIGURE 11. Various possible crystallization paths starting with the melt composition found in chromite-hosted melt inclusions (solid triangle). Open diamonds represent the path of crystallization if only chromite crystallized from this melt. The open circles represent the crystallization path assuming only olivine crystallized from this melt. Open diamonds represent a 50-50 mix of chromite and olivine crystallization from this starting composition. The solid circle represents the composition of a rehomogenized olivine-hosted melt inclusion. It is not possible to form a liquid line-of-descent from the chromite-hosted melt inclusion to the olivine-hosted melt inclusion through crystallization of olivine and chromite alone. The star represents a corrected olivine composition assuming the high P_2O_5 and CaO concentrations are due to secondary phosphate contamination.

sions could have obtained MgO contents higher than chromite without significant reequilibration of the host olivine that we have established was unlikely. The Cr_2O_3 of early ALH 77005 melts appears to have been underestimated in previous studies possibly because the abundance of chromite in trapped melts was underestimated. As chromite incorporates, Fe, Mg, Al, and Ti—in addition to Cr—it is important to accurately account for the trapped chromite found in melt inclusions when estimating melt inclusion bulk compositions. In addition, small increases in Cr_2O_3 in a magma have significant effects on the stability field of olivine and spinel, which expand at the expense of pyroxene and plagioclase (Onuma and Tohara 1983). Therefore, underestimating Cr_2O_3 can significantly impact models that estimate where minerals are likely to appear on the liquidus.

Our P_2O_5 concentrations in olivine-hosted melt inclusions, although showing considerable variability at higher MgO concentrations, are also considerably higher (~2.5 ± 1 wt% P_2O_5 at 6 wt% MgO) than those calculated by previous studies (~1 wt%). Regardless of the cause of the CaO and P_2O_5 enrichment, prior studies have underestimated the role of phosphates when calculating their compositions. This observation has significant implications for the REE signatures analyzed in olivine-hosted melt inclusions as the REE may reflect the phosphates contained in the inclusions and not the magmatic composition.

One final point can be made from looking at the olivine-hosted melt inclusions. It has been suggested that the two different types of magmatic olivine-hosted melt inclusions (Fig. 2) described earlier were produced by differences in their trapped melt composition, assimilation of crustal rocks, silicate immiscibility, and/or magma mixing (Jagoutz 1989; Harvey et al. 1993; Ikeda 1998). Some of these models also explained the high SiO_2 content determined for the melt inclusions. The results of our work show that the two types of melt inclusions have the same SiO_2 contents after rehomogenization. In fact, all the major and minor elements are similar in the fully rehomogenized melt inclusions, with the exception of P_2O_5. Several other possibilities exist to explain the physical differences in these melt inclusions. First, they may have been trapped at different stages of magmatic evolution. Second, they could have had different initial trapped volatile contents. Finally, they may have evolved differently due to differences in their cooling rate. However with the exception of CaO and P_2O_5, the melt inclusion analyses of this study do not support a conclusion that these melt inclusions are fundamentally different in their trapped melt composition.

TABLE 6. Prior studies of olivine-hosted melt inclusion compositions in ALH 77005 and estimates of the parental composition of LEW 88516

Sample	ALH 77005 MI	ALH 77005 MI	ALH 77005 MI	LEW Parental
SiO_2	49.94	63.6	53.9	53.72–54.89
TiO_2	2.81	0.91	0.92	0.06–0.86
Al_2O_3	11.89	16.6	10.69	6.06–9.27
Cr_2O_3	0.20	0.03	0.02	
FeO	14.66	3.62	9.39	12.58–15.72
MnO	0.42	0.1	0.25	
MgO	7.59	1.41	12.67	9.33–12.43
CaO	9.73	10.63	9.44	7.83–11.55
Na_2O	2.30	2.35	1.72	1.05–0.91
P_2O_5	1.12	1.44	0.48	
K_2O	0.12	0.17	0.52	0.05–0.09
Mg number	47	41	71	
Total	100.76	100.86	100.00	98.11–98.36
Reference	This study	Jagoutz (1989)	Ikeda (1998)	Harvey et al. (1993)
Method	rehomogenized	wide beam electron microprobe	calculated	calculated

The parental magma of ALH 77005 compared with other SNC meteorites

We have compared the rehomogenized olivine-hosted melt inclusions and the parental melt determined from chromite-hosted melt inclusions with studies of melt inclusions in two other classes of Martian meteorites, chassignites and nahklites (Table 7; see Fig. 12). Chassignites, which are dunites with >93% olivine, are thought to be cumulates (Floran et al. 1978). Varela et al. (2000) rehomogenized olivine-hosted melt inclusions in Chassigny using a heating stage. The melt inclusion composition determined by Varela et al. (2000) is very close to the evolved composition we determined from partially rehomogenized melt inclusions in ALH 77005. That they obtained olivine-hosted melt inclusions with compositions in excess of 69 wt% SiO_2 seems to indicate that they were not analyzing a parental melt for Chassigny and this composition will not be considered further. Using modal data and phase compositions, Johnson et al. (1991) constrained olivine-hosted melt inclusion compositions in Chassigny. The melt in equilibrium with Fo_{68} olivine is identified as the Chassigny A* composition and is slightly lower in MgO than the parental melt of ALH 77005. Like the olivines found in ALH 77005, if A* is projected to higher MgO, assuming the parental melt experienced olivine crystallization, Al_2O_3 is significantly lower and FeO is significantly higher than ALH 77005 suggesting a source composition that is different from that found in the chromites in ALH 77005.

Three melt inclusion rehomogenization studies have been performed on nakhlites (Varela et al. 2001; Rutherford et al. 2005; Stockstill et al. 2005), which contain high-Ca pyroxene and olivine in a fine-grained groundmass that makes up 25–60% of the rock (e.g., Treiman et al. 2005). The phenocryst compositions are essentially identical in the different nakhlites. Rehomogenization experiments on nakhlites MIL 03346 were performed in the same manner as those in our study (Rutherford et al. 2005). The compositions of the melt inclusions in olivine and high-Ca pyroxene are identical to the interstitial melt at the conditions of complete melt inclusion rehomogenization (very low Al_2O_3 and high FeO at 3.5–4.0 wt% MgO). This finding suggests that no significant fractionation affected the magma after melt inclusion entrapment. Stockstill et al. (2005) and Varela et al. (2001) both utilized heating stages to rehomogenize melt inclusions in Nakhla. The composition for Nakhla determined by Varela et al. (2001) is higher in SiO_2 and Al_2O_3 but lower in FeO than that reported in Stockstill et al. (2005). A projection line drawn through the rehomogenized melt inclusions analyzed for MIL 03346 is consistent with a melt inclusion composition determined by Stockstill et al. (2005). Therefore, we compare the parental melt of ALH 77005 with the Nahklite compositions determined from the studies of Stockstill et al. (2005) and Rutherford et al. (2005). If projected to the same MgO composition as ALH 77005 chromite-hosted melt inclusions, the Nahklite parent melts would be substantially lower in Al_2O_3 and SiO_2 and higher in FeO, than either the chromite-hosted melt inclusions but also the olivine-hosted melt inclusion compositions found in ALH 77005 and in

TABLE 7. Prior studies of magmatic compositions from other SNC meteorites

Meteorite	Chassigny (Chassignite)	Chassigny (A*) (Chassignite)	Yamato 980459 (Basaltic Shergottite)	MIL 03346 (Nahklite)	Nahkla (Nahklite)	Nahkla (Nahklite)
SiO_2	69.1	51.52	49.40	49.34	47.2	55.4
TiO_2	0.12	1.58	0.48	1.35	0.88	1.1
Al_2O_3	16.7	8.72	6.00	9.2	5.9	9.4
Cr_2O_3	0.00	–	0.71	0.03	–	0.2
FeO	3.12	19.02	15.80	22.89	26.9	13.4
MnO	0.07	0.53	0.43	0.44	0.71	0.2
MgO	1.32	7.08	18.10	3.51	4.6	4.9
CaO	1.24	8.49	7.20	9.35	10.1	10.2
Na_2O	4.11	2.29	0.80	2.58	2.3	3.2
P_2O_5	–	–	0.31	0.59	0.09	0.3
K_2O	3.33	0.77	0.02	0.73	0.39	0.6
Mg number	43	40	67	21	23	39
Total	99.1		99.54	100.01	99.1	98.9
Reference	Varela et al. (2000)	Johnson et al. (1991)	Dalton et al. (2005)	Rutherford et al. (2005)	Stockstill et al. (2006)	Varela et al. (2001)
Method	rehomogenized	calculated	bulk	rehomogenized	rehomogenized	rehomogenized (mean of 6)

Note: In cases where more than one melt inclusion composition was reported in the original study, the most primitive (lowest SiO_2) content is reported here.

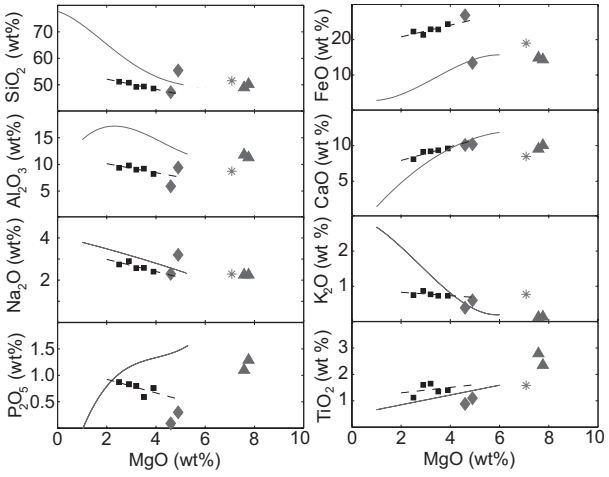

FIGURE 12. Comparison of the melt composition for rehomogenized olivine-hosted melt inclusions in ALH 77005 with other martian meteorites. Triangles are chromite-hosted melt inclusions suggested to represent the parental melt compostion of ALH 77005. The solid line is a fitted curve to ALH 77005 melt inclusions. Rehomogenized melt compositions for Nahkla are shown as diamonds (Stockstill et al. 2005). Rehomogenized melt compositions from primitive Nahklite MIL 00346 are plotted as squares (Rutherford et al. 2005). The A* composition determined from Chassigny melt inclusions is shown as an asterisk (Johnson et al. 1991).

Chassigny. This difference indicates that the source region of the nakhlites is significantly depleted in Al-bearing phases relative to source region of ALH 77005. It is also notable that the P_2O_5 in the Nakhla and MIL 03346 melts is quite low relative to the amounts determined for ALH 77005. However, both Varela et al. (2001) and Stockstill et al. (2005) presented a wide range of P_2O_5 concentrations, up to 1 wt%.

ACKNOWLEDGMENTS

The authors thank L. Danyushevsky, C. Goodrich, J. Longhi, and A. Treiman, along with an anonymous reviewer for their insightful comments that greatly improved this manuscripts. In addition we thank P. Hess, J. Longhi, and J. Devine for helpful discussions throughout the progress of this work. This work was supported by the following grant: NNX07AI50G.

REFERENCES CITED

Boctor, N.Z., D'Alexander, C.M.O., Wang, J., and Hauri, E. (2003) The sources of water in Martian meteorites: Clues from hydrogen isotopes. Geochimica et Cosmochimica Acta, 67, 3971–3989.

Borg, L.E. and Draper, D.S. (2003) A petrogenetic model for the origin and compositional variation of the Martian basaltic meteorites. Meteoritics and Planetary Science, 38, 1713–1731.

Borg, L.E., Nyquist, L.E., Wiesmann, H., and Reese, Y. (2002) Constraints on the petrogenesis of Martian meteorties from the Rb-Sr and Sm-Nd isotopic systematics of the lherzolitic shergottites ALH 77005 and LEW 88516. Geochimica et Cosmochimica Acta, 66, 2037–2053.

Danyushevsky, L.V., Della-Pasqua, F.N., and Sokolov, S. (2000) Reequilibration of melt inclusions trapped by magnesian olivine phenocrysts from subduction-related magmas: petrological implications. Contributions to Mineralogy and Petrology, 138, 68–83.

Danyushevsky, L.V., McNeill, A.W., and Sobolev, A.V. (2002) Experimental and petrological studies of melt inclusions in phenocrysts from mantle-derived magmas: an overview techniques, advantages and complications. Chemical Geology, 183, 5–24.

Edmunson, J., Borg, L.E., Shih, C.Y., and Papike, J.J. (2005) Defining the mechanisms that disturb the Sm-Nd isotopic systematics of the Martian meteorites: Examples from Dar al Gani 476 and Allan Hills 77005. Meteoritics and Planetary Science, 40, 1159–1174.

Eugster, H.P. and Skippen, G.B. (1967) Igneous and metamorphic reactions involving gas equilibria. In P.H. Abelson, Ed., Researches in Geochemistry, 2, p. 492–520. John Wiley and Sons, Inc., New York.

Floran, R.J., Prinz, M., Hlava, P.F., Keil, K., Nehru, C.E., and Hinthorne, J.R. (1978) The Chassigny meteorite: A cumulate dunite with hydrous amphibole-bearing melt inclusions. Geochimica et Cosmochimica Acta, 42, 1213–1219.

Frezzotti, M.-L. (2001) Silicate-melt inclusions in magmatic rocks: Applications to petrology. Lithos, 55, 273–299.

Gaetani, G.A. and Watson, E.B. (2000) Open system behavior of olivine-hosted melt inclusions. Earth and Planetary Science Letters, 183, 27–41.

——— (2002) Modeling the major-element evolution of olivine-hosted melt inclusions. Chemical Geology, 183, 25–41.

Ganguly, J. and Tazzoli, V. (1994) Fe^{2+}-Mg interdiffusion in orthopyroxene: Retrieval from the data on intracrystalline exchange reaction. American Mineralogist, 79, 930–937.

Goodrich, C.A. and Harvey, R.P. (2002) The parent magmas of lherzolitic shergottites ALH 77005 and LEW 88516: A reevaluation from magmatic inclusions in olivine and chromite. 65th Annual Meteoritical Society Meeting, Abstract no. 5123.

Harrison, T.M. and Watson, E.B. (1984) The behavior of apatite during crustal anatexis: Equilibrium and kinetic considerations. Geochimica et Cosmochimica Acta, 48, 1467–1477.

Harvey, R.P., Wadhwa, M., McSween, H.Y., and Crozaz, G. (1993) Petrography, mineral chemistry, and petrogenesis of Antarctic Shergottite LEW88516. Geochimica et Cosmochimica Acta, 57, 4769–4783.

Hauri, E. (2002) SIMS analysis of volatiles in silicate glasses, 2: isotopes and abundances in Hawaiian melt inclusions. Chemical Geology, 183, 115–141.

Herd, C.D.K., Borg, L.E., Jones, J.H., and Papike, J.J. (2002) Oxygen fugacity and geochemical variations in the Martian basalts: Implications for Martian basalt petrogenesis and the oxidation state of the upper mantle of Mars. Geochimica et Cosmochimica Acta, 66, 2025–2036.

Ikeda, Y. (1994) Petrography and petrology of the ALH-77005 shergottite. Proceedings of the NIPR Symposium on Antarctic Meteorites, 7, p. 9–29.

——— (1998) Petrology of magmatic silicate inclusions in the Allan Hills 77005 lherzolitic shergottite. Meteoritics and Planetary Science, 33, 803–812.
Jagoutz, E. (1989) Sr and Nd isotopic systematics in ALHA 77005: Age of shock metamorphism in shergottites and magmatic differentiation on Mars. Geochimica et Cosmochimica Acta, 53, 2429–2441.
——— (1991) Chronology of SNC meteorites. Space Science Reviews, 56, 13–22.
Jarosewich, E., Nelen, J.A., and Norber, J.A. (1979) Electron microprobe reference samples for mineral analyses. Smithsonian Contributions to the Earth Sciences, 22, 68–72.
Johnson, M.C., Rutherford, M.J., and Hess, P.C. (1991) Chassigny petrogenesis: Melt compositions, intensive parameters, and water contents of Martian magmas. Geochimica et Cosmochimica Acta, 55, 349–366.
Jurewicz, A.J.G. and Watson, E.B. (1988) Cations in olivine, Part 2: Diffusion in olivine xenocrysts, with applications to petrology and mineral physics. Contributions to Mineralogy and Petrology, 99, 186–201.
Kamenetsky, V. (1996) Methodology for the study of melt inclusions in Cr-spinel, and implications for parental melts of MORB from FAMOUS area. Earth and Planetary Science Letters, 142, 479–486.
Longhi, J. and Pan, V. (1989) The parent magmas of the SNC meteorites. 19th Lunar and Planetary Science Conference, p. 451–464. Lunar and Planetary Institute, Houston, Texas.
Lundberg, L., Crozaz, G., and McSween, H.Y. (1990) Rare earth elements in minerals of the ALHA 77005 shergottite and implications for its parent magma and crystallization history. Geochimica et Cosmochimica Acta, 54, 2535–2547.
McCallum, I.S. (1996) The Stillwater Complex. In R.G. Cawthorn, Ed., Layered intrusions, p. 441–484. Elsevier Science, Amsterdam.
McCoy, T.J., Taylor, G.J., and Keil, K. (1992) Zagami: Product of a two stages magmatic history. Geochimica et Cosmochimica Acta, 56, 3571–3582.
McSween, H.Y. (1985) SNC meteorites: Clues to Martian petrologic evolution. Reviews of Geophysics, 23, 391–416.
McSween, H.Y., Lundberg, L., and Crozaz, G. (1987) Crystallization of the ALHA77005 Shergottite: How closed is a closed system? LPSC XIX, p. 766–767 (abstract). Lunar and Planetary Institute, Houston, Texas.
McSween, H.Y., Taylor, L.A., and Stolper, E.M. (1979) Allan Hills 77005: A new meteorite type found in Antarctica. Science, 204(4398), 1201–1203.
Milman-Barris, M.S., Beckett, J., Baker, M.B., Morgan, Z., Hofmann, A.E., Crowley, M.R., Vielzeuf, D., and Stolper, E.M. (2008) Zoning of phosphorus in igneous olivine. Contributions to Mineralogy and Petrology, 155, 739–765.
Morse, S.A. (1994) Basalts and Phase Diagrams, 493 p. Krieger Publishing Company, Malabar, Florida.
Mysen, B. (1975) Partition of iron and magnesium between crystals and partial melts in peridotite upper mantle. Contributions to Mineralogy and Petrology, 52, 69–76.
Onuma, K. and Tohara, T. (1983) Effect of chromium on phase relations in the join forsterite-anorthite-diopside in air at 1 Atm. Contributions to Mineralogy and Petrology, 84, 174–181.
Roedder, E. (1984) Fluid Inclusions, 12, 646 p. Reviews in Mineralogy (Monograph), Mineralogical Society of America, Chantilly, Virginia.
Roeder, P.L. (1974) Activity of iron and olivine solubility in basaltic liquids. Earth and Planetary Science Letters, 23, 397–410.
Rutherford, M.J., Calvin, C.L., Nicholis, M., and McCanta, M. (2005) Petrology and melt compositions in Nakhlite MIL-03346: Significance of data from natural sample and from experimentally fused groundmass and M.I.'s. LPSC XXXVI, p. 2233 (abstract). Lunar and Planetary Institute, Houston, Texas.
Sobolev, A.V., Dmitriyev, L.V., Barsukov, V.L., Nevsorov, V.N., and Slutskiy, A.B. (1980) The formation conditions of the high-magnesium olivines from the monomineralic fraction of Luna 24 regolith. Proceedings of the Lunar Planetary Science Conference XI, 1, 105–116.
Stockstill, K.R., Bodnar, R.J., McSween, H.Y., and Lentz, R.C.F. (2002) Melt inclusions in SNC meteorites as indicators of parental melts on Mars. LPSC XXXIII, p. 1644 (abstract). Lunar and Planetary Institute, Houston, Texas.
Stockstill, K.R., McSween, H.Y., and Bodnar, R.J. (2005) Melt inclusions in augite of the Nakhla Martian meteorite; Evidence for basaltic parental melt. Meteoritics and Planetary Science, 40, 377–396.
Treiman, A.H. (1986) The parental magma of the Nahkla achondrite: Ultrabasic volcanism on the Shergottite Parent Body. Geochimica et Cosmochimica Acta, 50, 1061–1070.
——— (2003) Chemical compositions of Martian basalts (shergottites): Some inferences on basalt formation, mantle metasomatism, and differentiation in Mars. Meteoritics and Planetary Science, 38, 1849–1864.
——— (2005) The nakhlite meteorites: Augite-rich igneous rocks from Mars. Chemie der Erde, 65, 203–270.
Ulmer, P. (1989) The dependence of the Fe^{2+}-Mg cation-partitioning between olivine and basaltic liquid on pressure, temperature, and composition. Contributions to Mineralogy and Petrology, 101, 261–273.
Varela, M.E., Kurat, G., Bonnin-Mosbah, M., Clocchiatti, R., and Massare, D. (2000) Glass-bearing inclusions in olivine of the Chassigny achondrite: Heterogeneous trapping at sub-igneous temperatures. Meteoritics and Planetary Science, 35, 39–52.
Varela, M.E., Kurat, G., and Clocchiatti, R. (2001) Glass-bearing inclusions in Nakhla (SNC meteorite) augite: Heterogeneously trapped phases. Mineralogy and Petrology, 71, 155–172.
Wadhwa, M. (2001) Redox State of Mars' Upper Mantle and Crust from Eu Anomalies in Shergottite Pyroxenes. Science, 291, 1527–1530.
Wadhwa, M., McSween, H.Y., and Crozaz, G. (1994) Petrogenesis of shergottite meteorites inferred from minor and trace element microdistributions. Geochimica et Cosmochimica Acta, 58, 4213–4229.
Watson, L.L., Hutcheon, I.D., Epstein, S., and Stolper, E.M. (1994) Water on Mars: Clues from deuterium/hydrogen and water contents of hydrous phases in SNC meteorites. Science, 265, 86–90.
Zapunnyy, S.A., Sobolev, A.V., Bogdanov, A.A., Slutskiy, A.B., Dmitriyev, L.V., and Kunin, L.L. (1989) An apparatus for high-temperature optical research with controlled oxygen fugacity. Geochemical International, 26, 120–128.
Zipfel, J. and Goodrich, C.A. (2001) REE in Melt Inclusions in olivine of ALHA77005. 54th Annual Meteoritical Society Meeting, p. 5192 (abstract), Vatican City, Italy.

MANUSCRIPT RECEIVED APRIL 1, 2007
MANUSCRIPT ACCEPTED JUNE 2, 2008
MANUSCRIPT HANDLED BY MARC HIRSCHMANN